REPORT DOCUMENTATION PAGE

Form Approved
OMB No. 0704-0188

1. REPORT DATE *(DD-MM-YYYY)*
20-10-2005

2. REPORT TYPE
Briefing Charts

3. DATES COVERED *(From - To)*

4. TITLE AND SUBTITLE

Ablation of Liquids for Laser Propulsion with TEA CO_2 Laser (Briefing Charts, PREPRINT)

5a. CONTRACT NUMBER

5b. GRANT NUMBER

5c. PROGRAM ELEMENT NUMBER

6. AUTHOR(S)
John Sinko, Lisa Kodgis, Simon Porter, Enrique Sterling, Jun Lin and Andrew V. Pakhomov (Dept of Physics, UA Huntsville); C. William Larson and Franklin B. Mead, Jr. (AFRL/PRSP)

5d. PROJECT NUMBER
4847

5e. TASK NUMBER
0159

5f. WORK UNIT NUMBER

7. PERFORMING ORGANIZATION NAME(S) AND ADDRESS(ES)

Air Force Research Laboratory (AFMC)
AFRL/PRSP
10 E. Saturn Blvd.
Edwards AFB CA 93524-7680

8. PERFORMING ORGANIZATION REPORT NUMBER

AFRL-PR-ED-VG-2005-395

9. SPONSORING / MONITORING AGENCY NAME(S) AND ADDRESS(ES)

Air Force Research Laboratory (AFMC)
AFRL/PRS
5 Pollux Drive
Edwards AFB CA 93524-70448

10. SPONSOR/MONITOR'S ACRONYM(S)

11. SPONSOR/MONITOR'S NUMBER(S)
AFRL-PR-ED-VG-2005-395

12. DISTRIBUTION / AVAILABILITY STATEMENT

Approved for public release; distribution unlimited

13. SUPPLEMENTARY NOTES
Presented at the 4th International Symposium on Beamed Energy Propulsion, Nara, Japan, 11-14 Nov 2005.

14. ABSTRACT
Time-resolved force sensing and intensified charge-coupled device (ICCD) imaging techniques were applied to the study of the force generation mechanism for laser ablation of liquids. A Transversely Excited at Atmospheric pressure (TEA) CO_2 laser operated at 10.6 μm, 300 ns pulse width, and 9 J pulse energy was used to ablate liquids contained in various aluminum and glass vessels. Net imparted impulse and coupling coefficient were derived from the force sensor data and relevant results will be presented for various container designs and liquids used. ICCD imaging was used in conjunction with the dynamic force techniques to examine dependencies on absorption depth, irradiance, surface curvature, and container geometry. ICCD imaging was also used to determine whether surface or volume absorption should be preferable for laser propulsion using liquid propellants. Finally, ballistic experiments were conducted in order to verify the dynamic force data and lend additional evidence as to the predominant methods of force generation.

15. SUBJECT TERMS

16. SECURITY CLASSIFICATION OF:			17. LIMITATION OF ABSTRACT	18. NUMBER OF PAGES	19a. NAME OF RESPONSIBLE PERSON
					Dr. Franklin B. Mead, Jr.
a. REPORT	**b. ABSTRACT**	**c. THIS PAGE**			**19b. TELEPHONE NUMBER** *(include area code)*
Unclassified	**Unclassified**	**Unclassified**	A	39	(661) 275-5929

Ablation of Liquids for Laser Propulsion with TEA CO_2 Laser (Preprint)

John Sinko, Lisa Kodgis, Simon Porter, Enrique Sterling, Jun Lin, and Andrew V. Pakhomov

The University of Alabama in Huntsville, Huntsville, AL 35899, USA

C. William Larson and Franklin B. Mead, Jr.

Propulsion Directorate, Air Force Research Laboratory, Edwards AFB, CA 93524-7680, USA

Acknowledgements

ERC, Inc.
Edwards AFB, CA 93524-7680, USA

Laser Propulsion Group
Adam Hendrickson, Casey Kemp, Jonathon Kemper, Jonathan Lassiter, Venkatakrishna Mukundaraj, Christopher Smith, and Wesley Swift, Jr.

UAH Department of Physics
The University of Alabama in Huntsville, Huntsville, AL 35899, USA

Gene Nelson
UAH Glassblower

Scott Anderson
Audio Arrangement

The University of Alabama in Huntsville

Outline

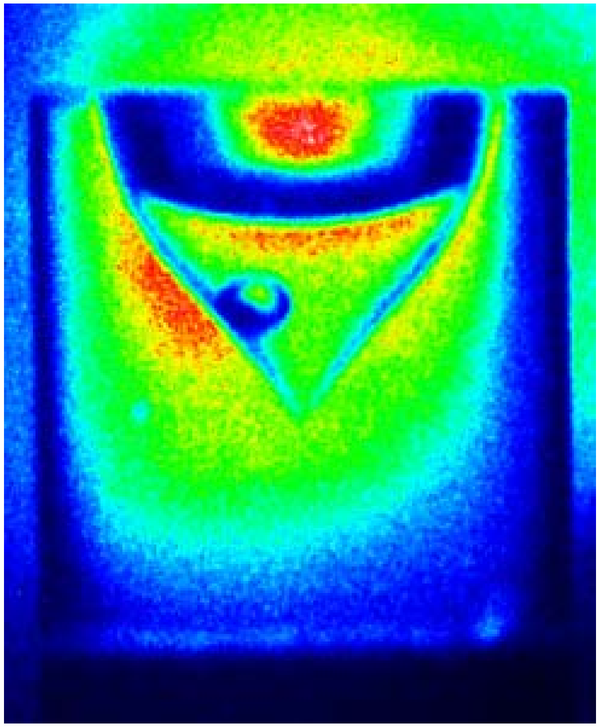

1. Introduction
2. Force
3. ICCD Ballistics
4. ICCD Imaging
5. Results and Discussion
6. Conclusions

Laser Ablation

- Laser Ablation: removal of material by any physical process under laser irradiation

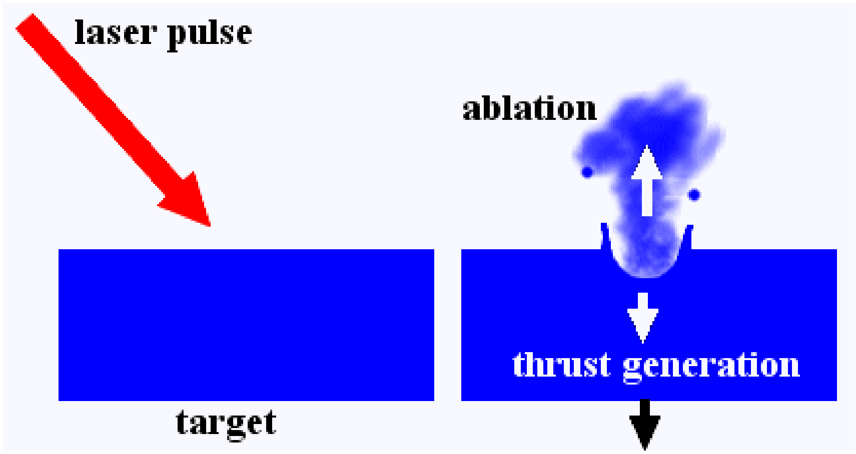

- Laser Ablation of Liquids
  - C_m up to 350 dyne/W
  - Irradiance: 10^7-10^8 W/cm^2
  - I_{sp} up to 50 s

Motivation

(1) What is the physical mechanism generating thrust during the laser ablation of a liquid?

- Plasma formation
- Vaporization
- Explosive boiling / Phase explosion
- Cavity collapse / splashing

(2) How do the ablation mechanisms for surface and volume-absorbing liquids differ?

(3) How does C_m depend on:

- Container geometry
- Liquid surface curvature
- Absorption depth

Force Experiments

The University of Alabama in Huntsville

Experimental Setup (Force Sensors)

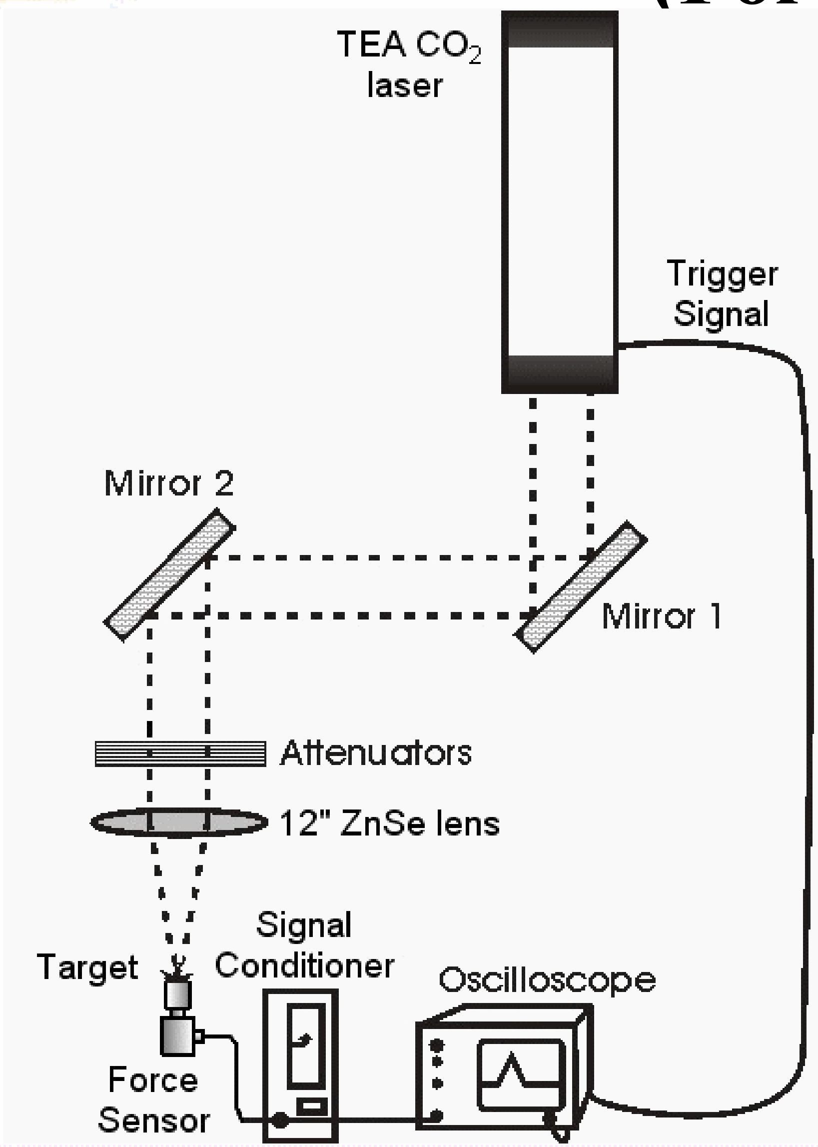

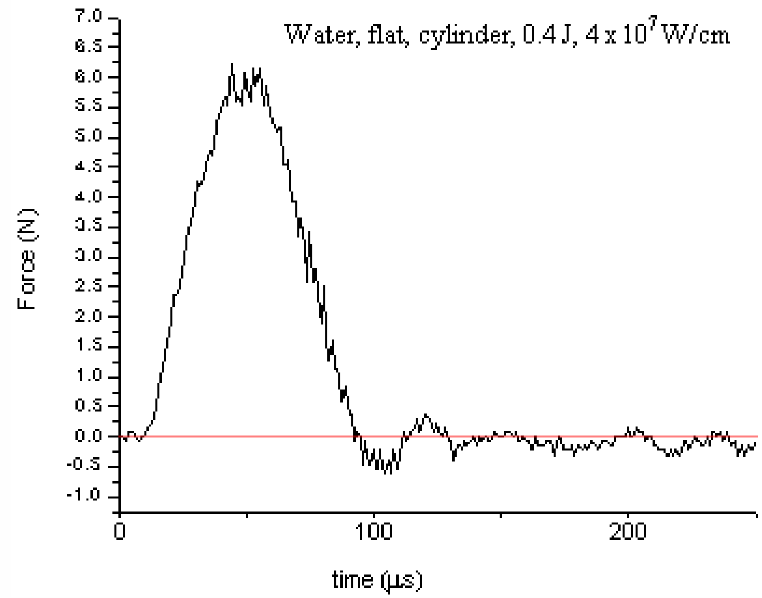

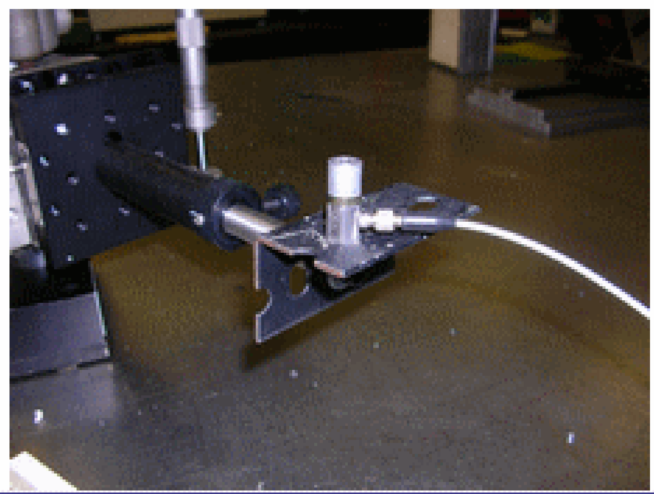

Piezoelectric Force Sensors

Small Force Sensor

- **Maximum Force: 9.786 N**
- Linearity: < 1%
- Sensitivity: 526.6 mV/N
- Discharge time constant: > 1.0 s
- Rise Time: 5 µs
- Resolution: 10^{-4} N

PCB-209C01

Large Force Sensor

- **Maximum Force: 444.8 N**
- Linearity: < 0.4%
- Sensitivity: 11.96 mV/N
- Discharge time constant: > 500 s
- Rise Time: 8 µs
- Resolution: 10^{-3} N

PCB-200B02

Force-Time Curve

- Measurements are as follows:
  - Single laser shot
  - Force vs. time
  - Large force peak observed (10-90 μs, centered 40-50 μs)

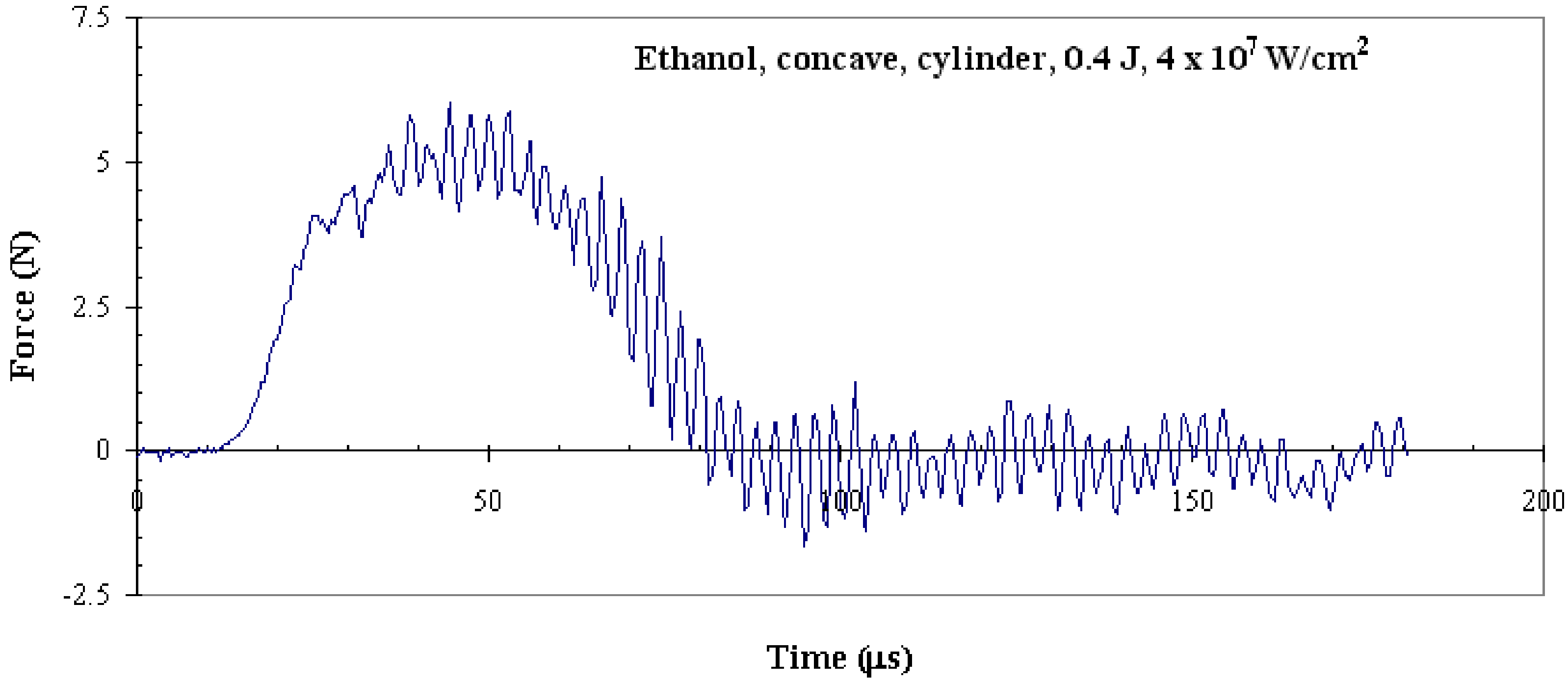

  - Integrate to find I, then derive C_m

Coupling Coefficients and Peak Force

Peak Force (N)		Hexane	Ethanol	Water
Cylinder	Flat	3.4 ± 0.4	5.2 ± 0.6	4.1 ± 0.4
	Concave	3.1 ± 0.2	6.0 ± 0.1	5.7 ± 0.5
Cone	Flat	3.6 ± 0.3	5 ± 1	4.1 ± 0.4
	Concave	3.7 ± 0.3	5.8 ± 0.4	5.3 ± 0.4

C_m (dyne/W)		Hexane	Ethanol	Water
Cylinder	Flat	22 ± 3	50 ± 3	43 ± 4
	Concave	22 ± 3	56 ± 4	60 ± 6
Cone	Flat	23 ± 1	49 ± 6	47 ± 5
	Concave	24 ± 3	56 ± 3	56 ± 6

(1.6×10^7 W/cm^2, 0.4 J, Force Sensor)

UAH
The University of Alabama in Huntsville

Surface Curvature

- Radius of Curvature R

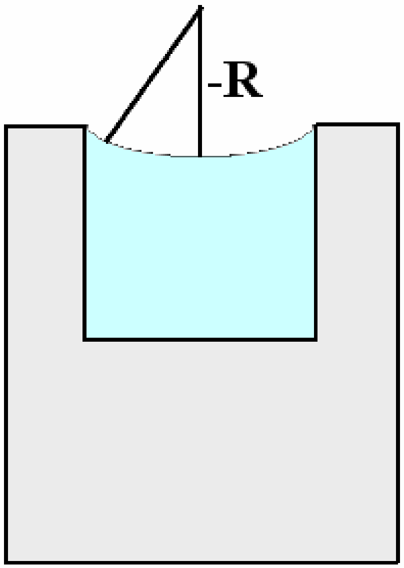

- Curvature κ (cm^{-1})

$$\kappa \equiv \frac{1}{R}$$

- C_m directly dependent on κ

Water, flat, cylinder, 0.4 J, 2 x 10^7 W/cm^2

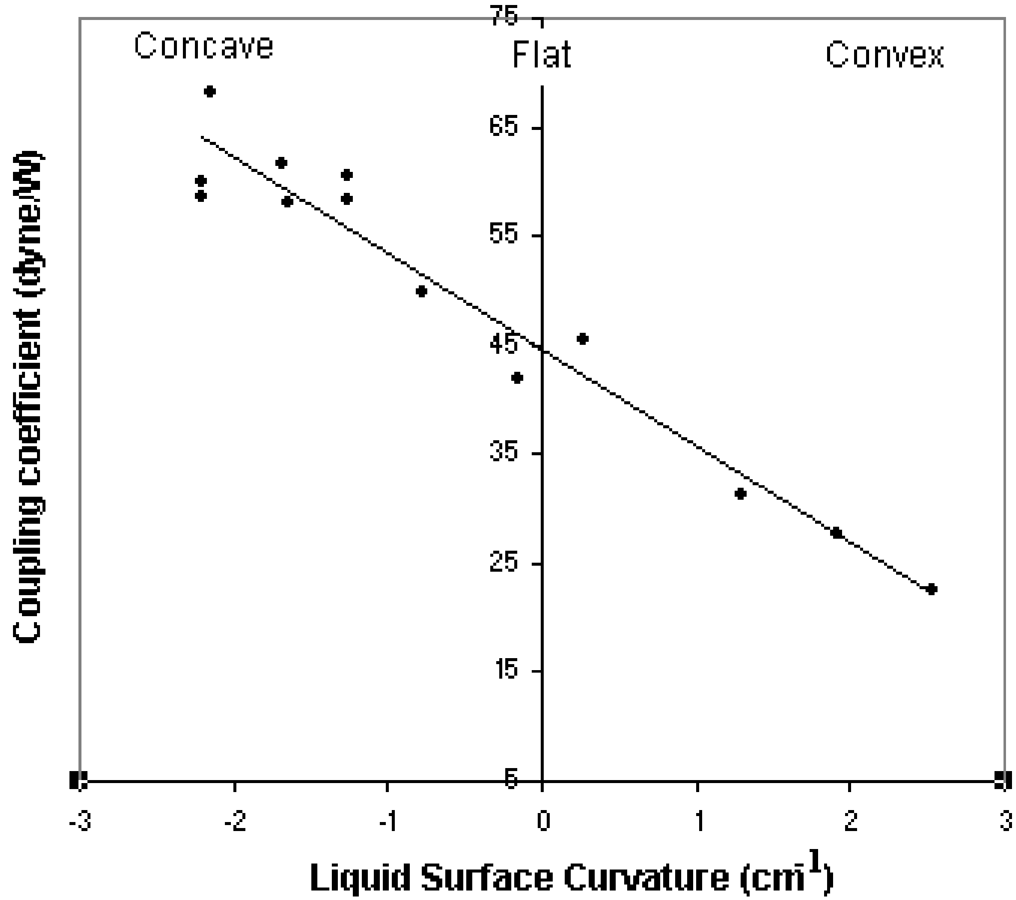

Imaging Experiments

ICCD Imaging

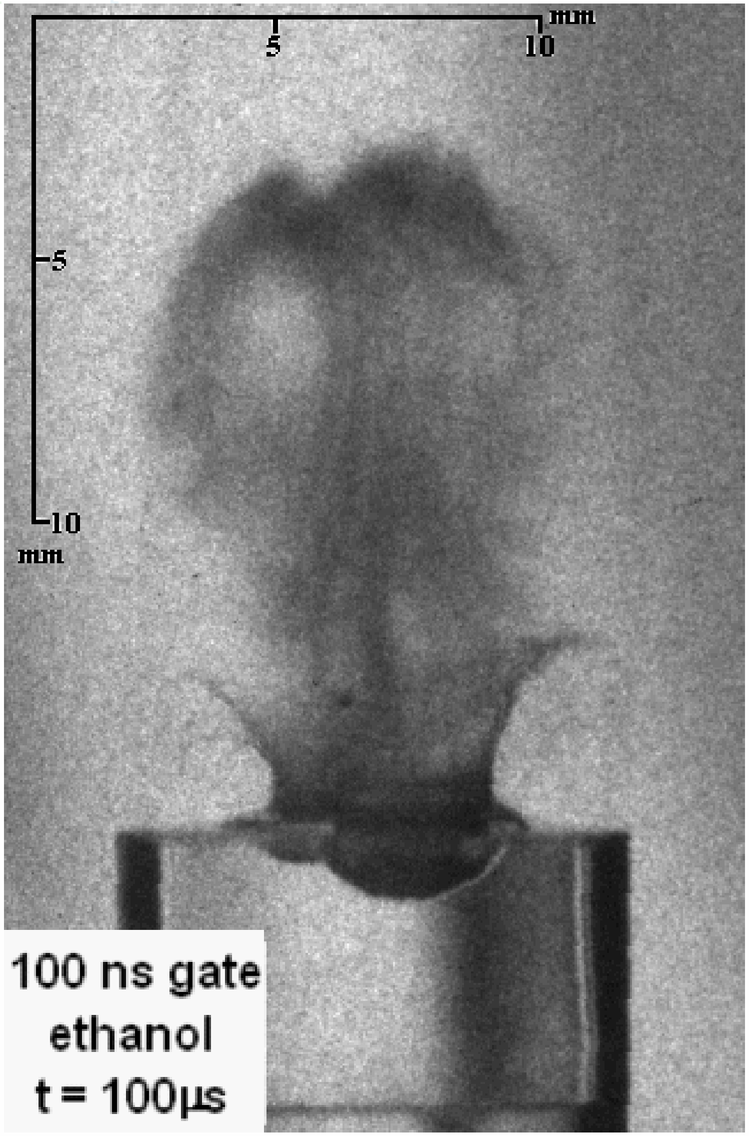

Information on:

Initial plume velocities

Cavity growth rates

Characteristic physical processes

Timeline of processes

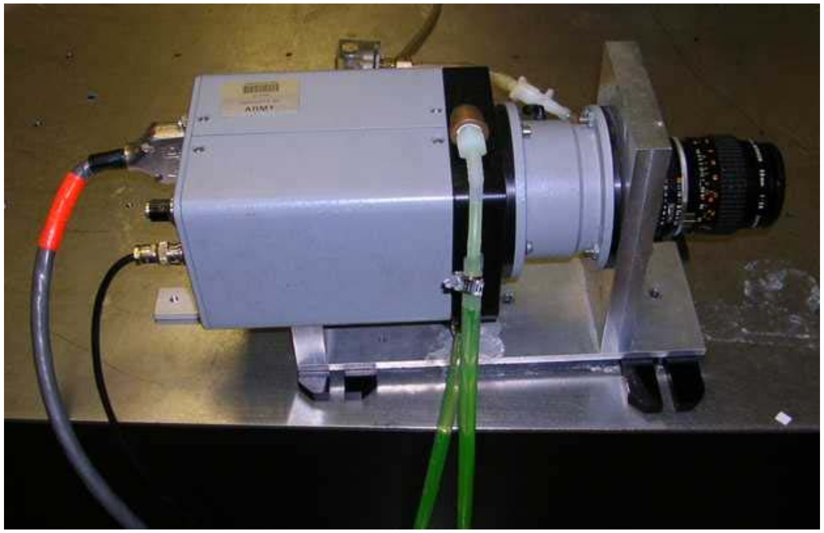

UAH
The University of Alabama in Huntsville

ICCD Ballistics Setup

- Gated CCD technique
- Single laser shot per image
- Highly repeatable
- Composite sequences

- 382 x 574 pixel images
- >5 ns gate width (exposure)
- 5 ns - 83 ms delay

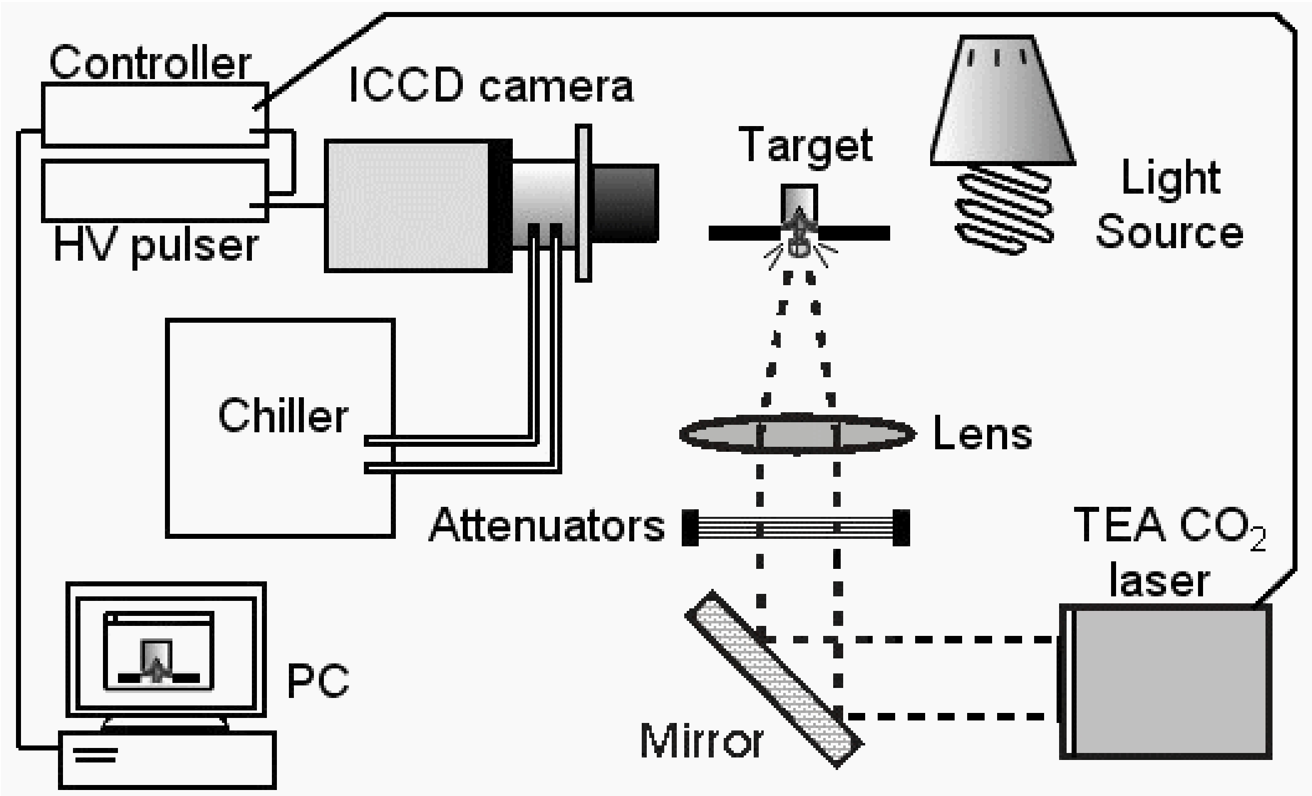

Coupling Coefficients, dyne/W

(Water, 3 mm^2 spot size)

Energy (J)	Irradiance (W/cm^2)	Small Force Sensor	Large Force Sensor	Ballistics
0.4	4×10^7	110 ± 14	-	98 ± 9
1.2	1×10^8	44 ± 24	53 ± 21	37 ± 5
3.6	5×10^8	-	14 ± 3	14 ± 2

$$C_m = \frac{I}{E_{pulse}} = \frac{m}{E_{pulse}} \sqrt{2\,g\,h_{max}}$$

Imaging Setup

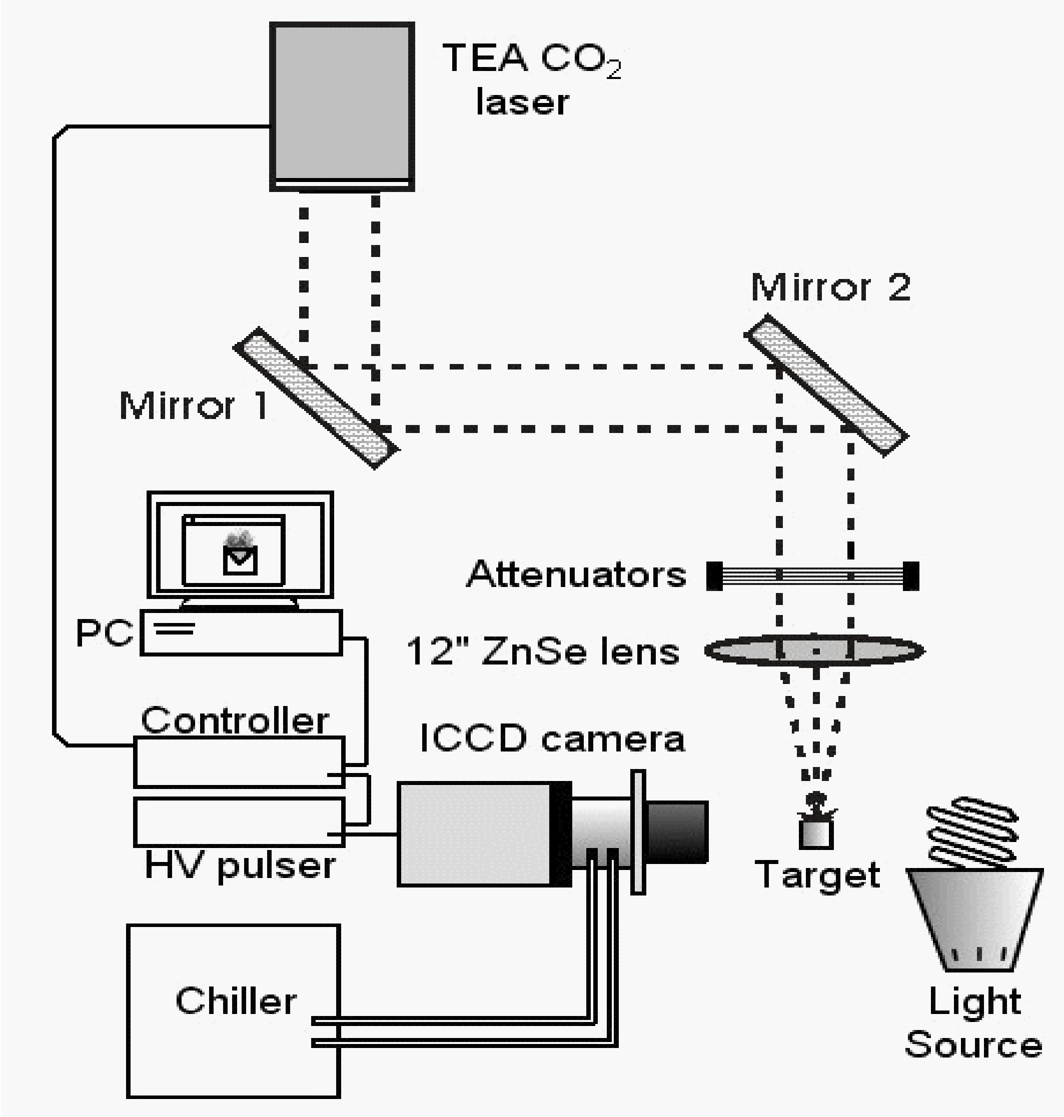

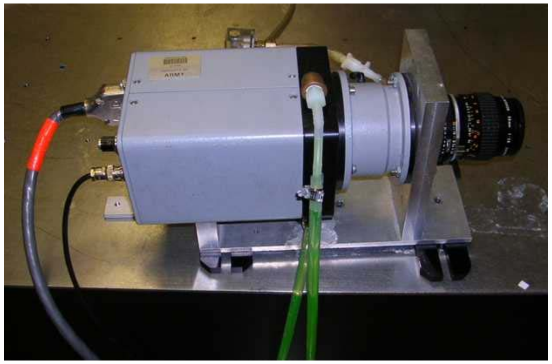

ICCD Images

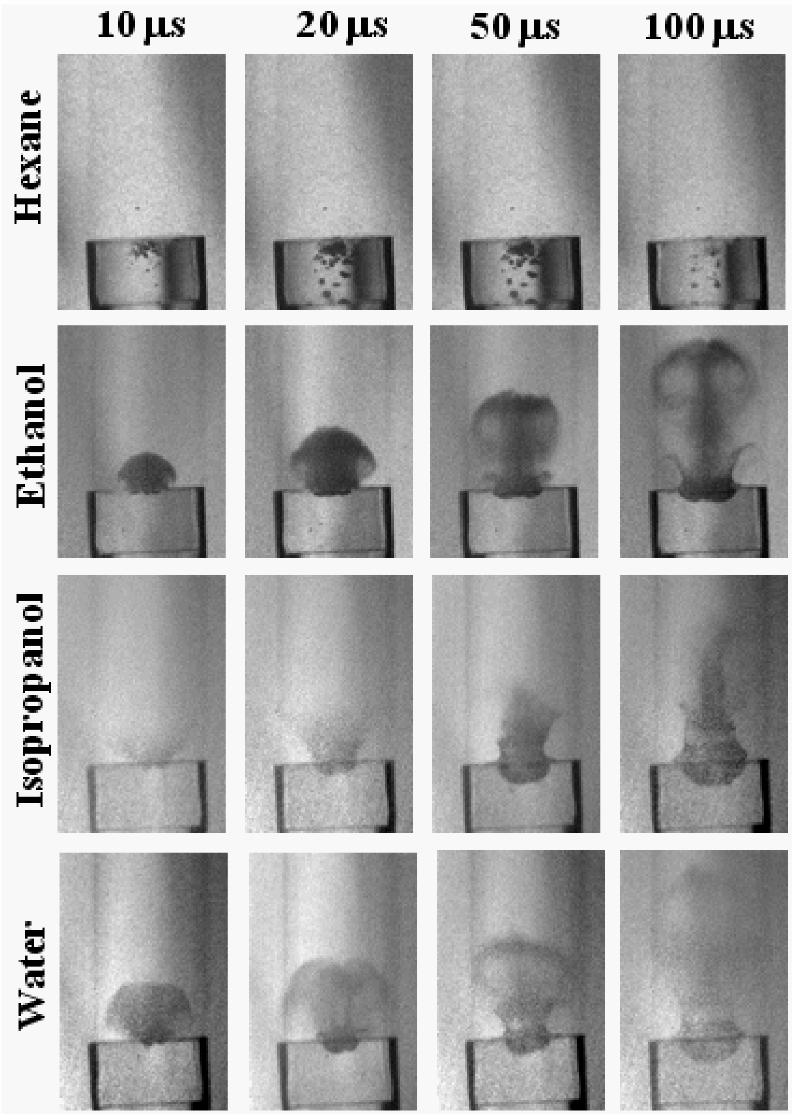

Volume-absorbing

(hexane)

- No observed plume
- No cavity formation
- Boiling

Surface-absorbing

(ethanol, isopropanol, water)

- Vapor plume
- Cavity formation

Surface Absorption

Ethanol, 0.4 J, 4 x 10^7 W/cm^2

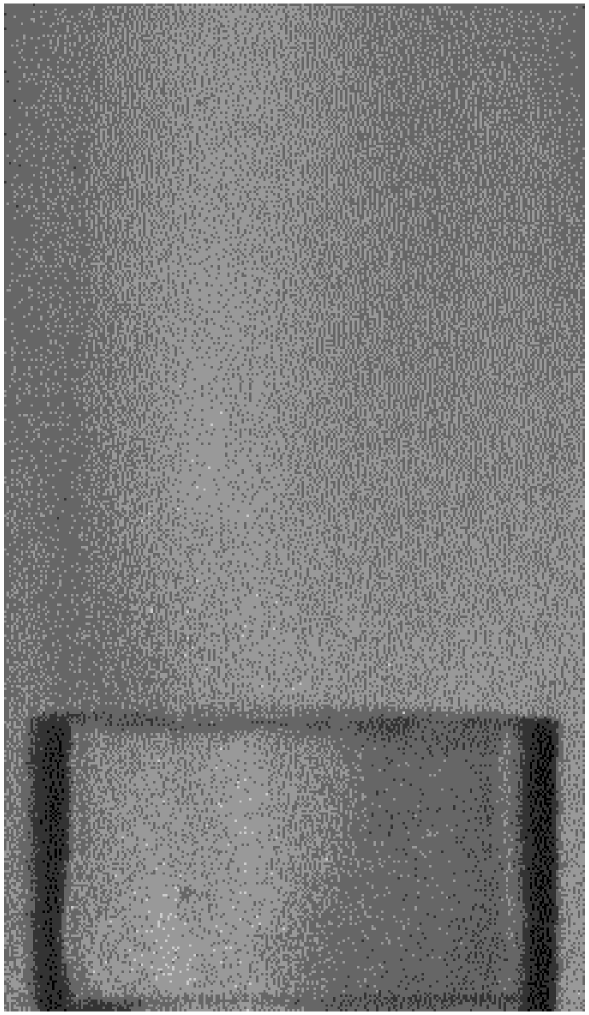

UAH

The University of Alabama in Huntsville

Volume Absorption (Hexane)

- 0.4 J
- 4 x 10^7 W/cm^2
- No plasma
- No cavity
- No plume
- Boiling

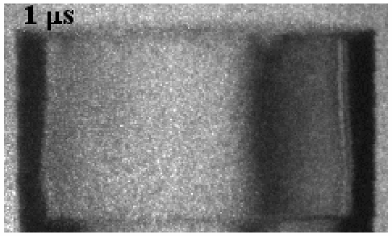

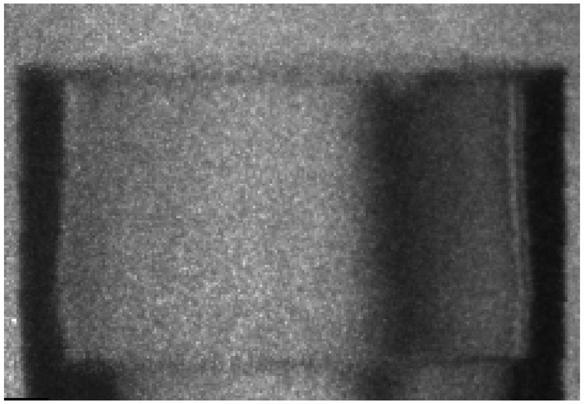

- 1.1 J
- 1 x 10^8 W/cm^2
- Plasma
- Surface cavity
- Vapor plume

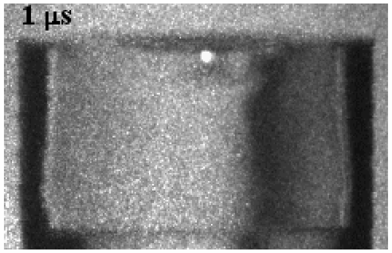

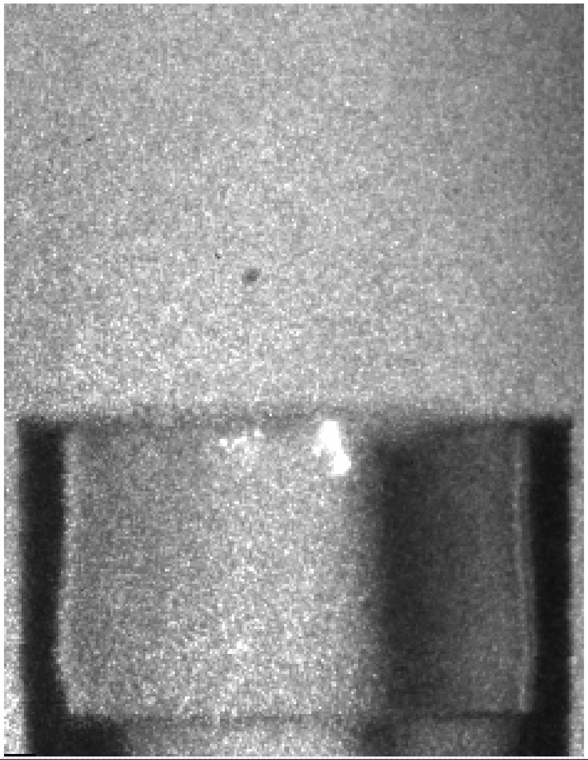

Containers: Cylinder vs. Cone

- Water, 10-100 μs
- Virtually no difference observed

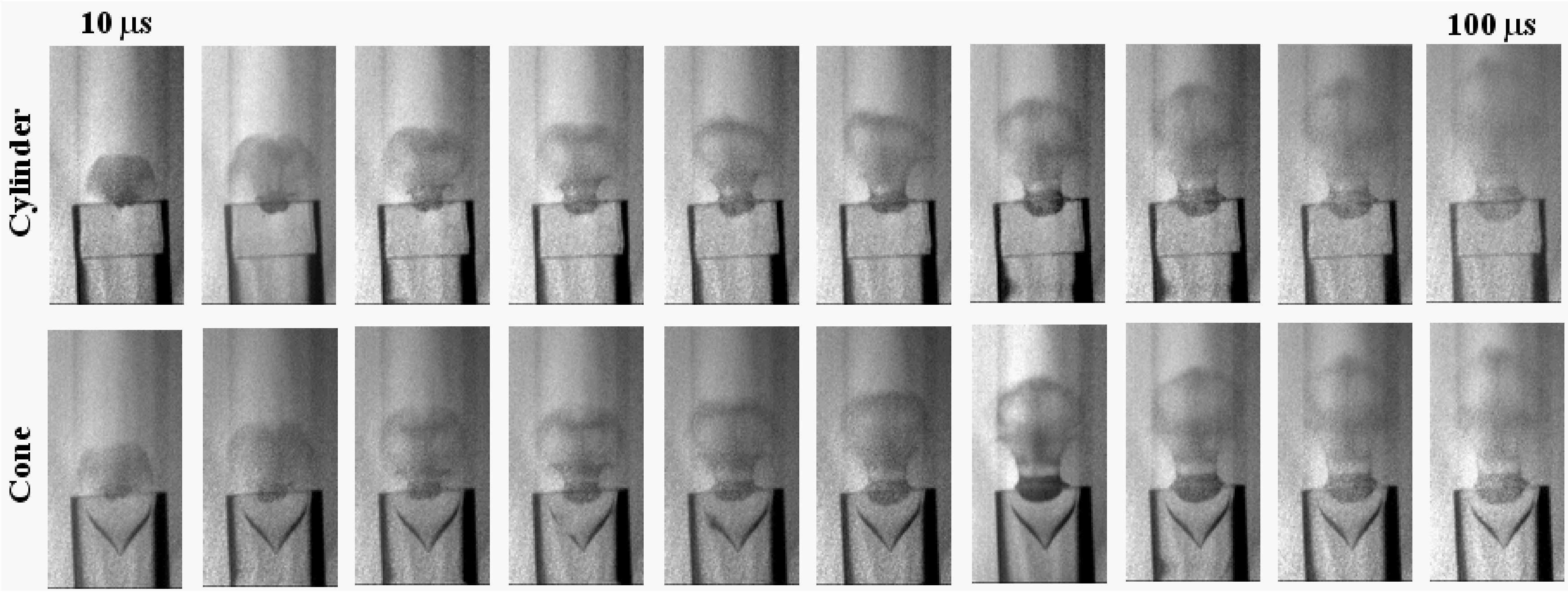

Surfaces: Flat vs. Concave

- Ethanol, 5-50 μs:

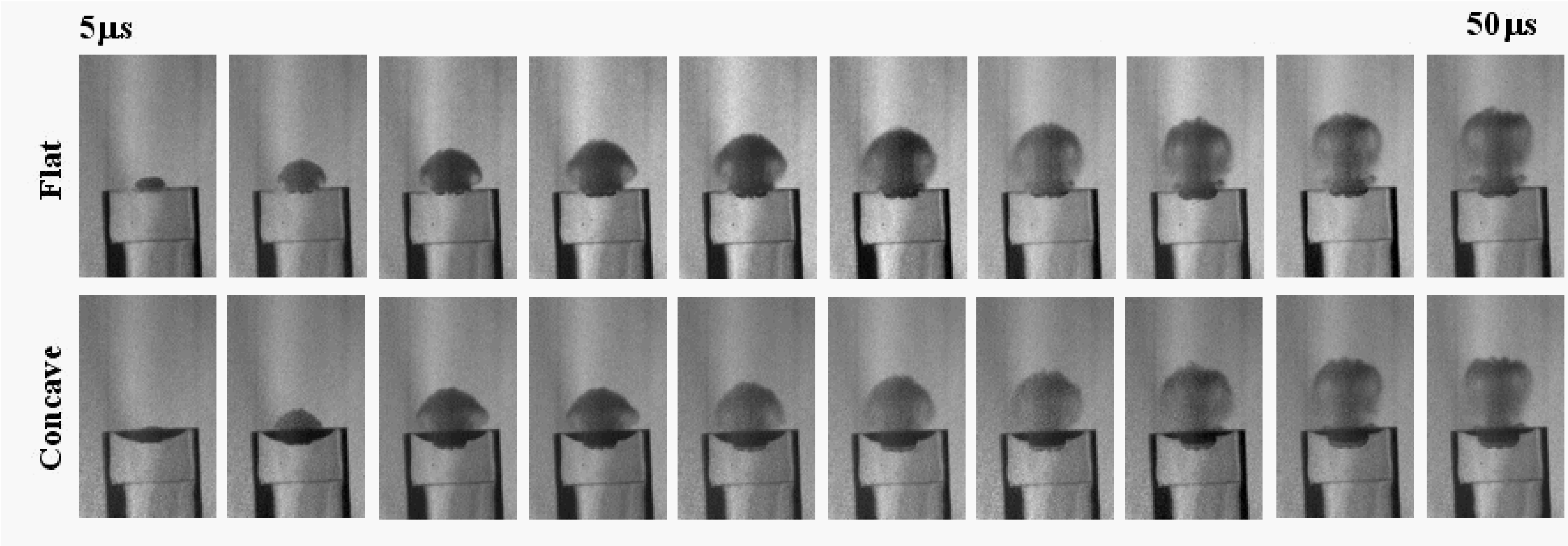

Effect of Initial Curvature (100 μs)

<u>Flat</u>:

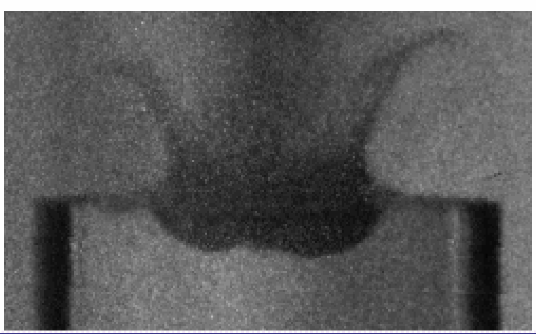

<u>Concave</u>:

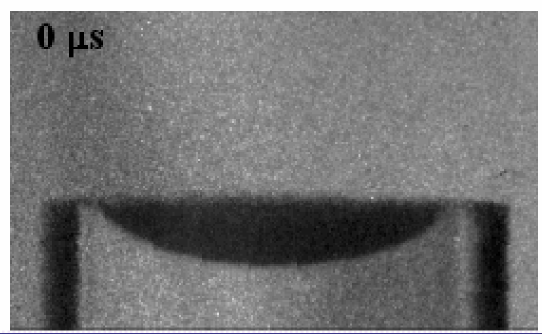

UAH
The University of Alabama in Huntsville

Analysis of Mass Loss and Cavity Growth

Model as oblate spheroid

$$\left(V = \frac{2}{3}\pi\, a\, b^2\right)$$

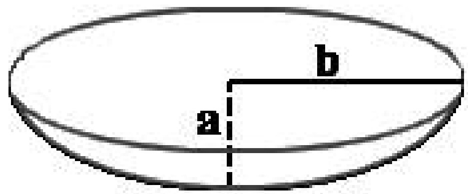

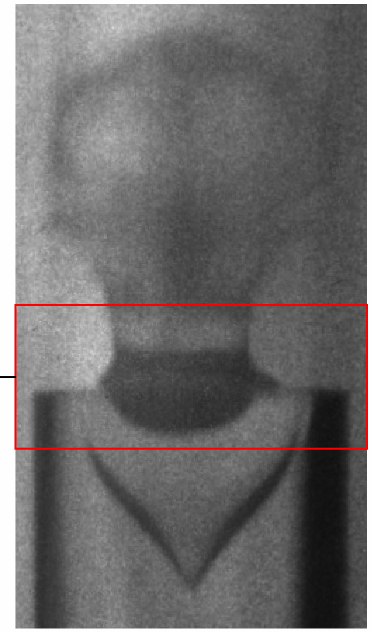

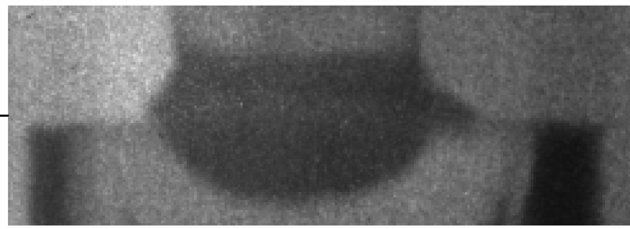

Correction for distortion

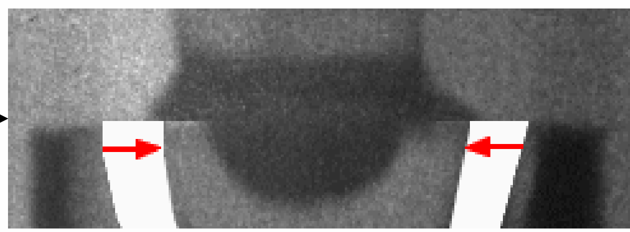

Subtraction of rim volume

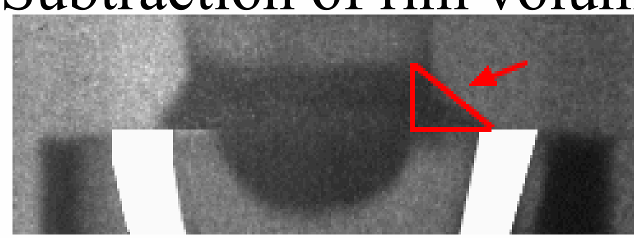

Cavity measurement

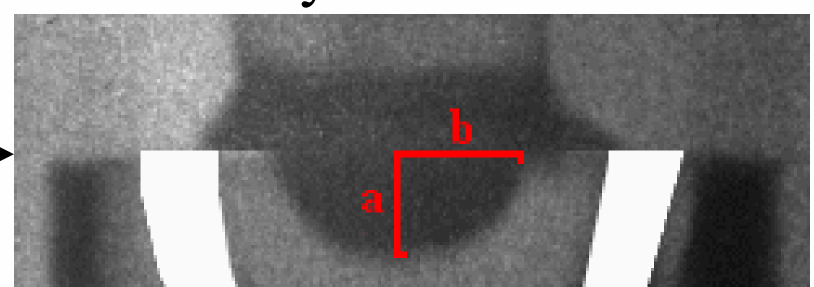

Liquid Mass Loss

- All data using cylinder, flat surface, 0.4 J, 7 x 10^7 W/cm^2
- Increased cavity growth during initial 100 µs
- ICCD imaging: Mass (mg) removed during initial 100 µs
- Scientific Balance: Total mass (mg) removed in entire process

Mass Loss (mg)

Liquid	Hexane	Ethanol	Isopropanol	Water
0-100 µs	0	2 ± 1	1 ± 1	1 ± 1
Total Process	4 ± 1	51 ± 6	51 ± 2	51 ± 5
Ratio	0 %	4 %	2 %	2 %

UAH
The University of Alabama in Huntsville

Analysis of Initial Velocities

Center plume front height h

Δh paired with known Δt

$$\lim_{t\to 0} \frac{\Delta h}{\Delta t} = v_0$$

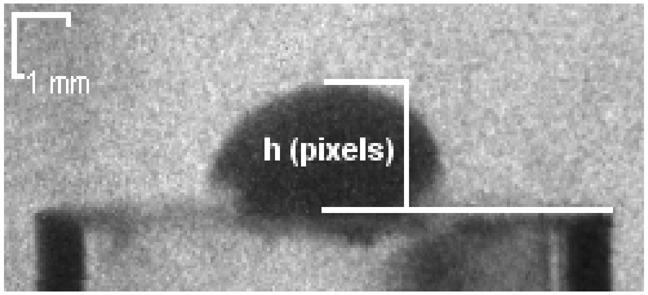

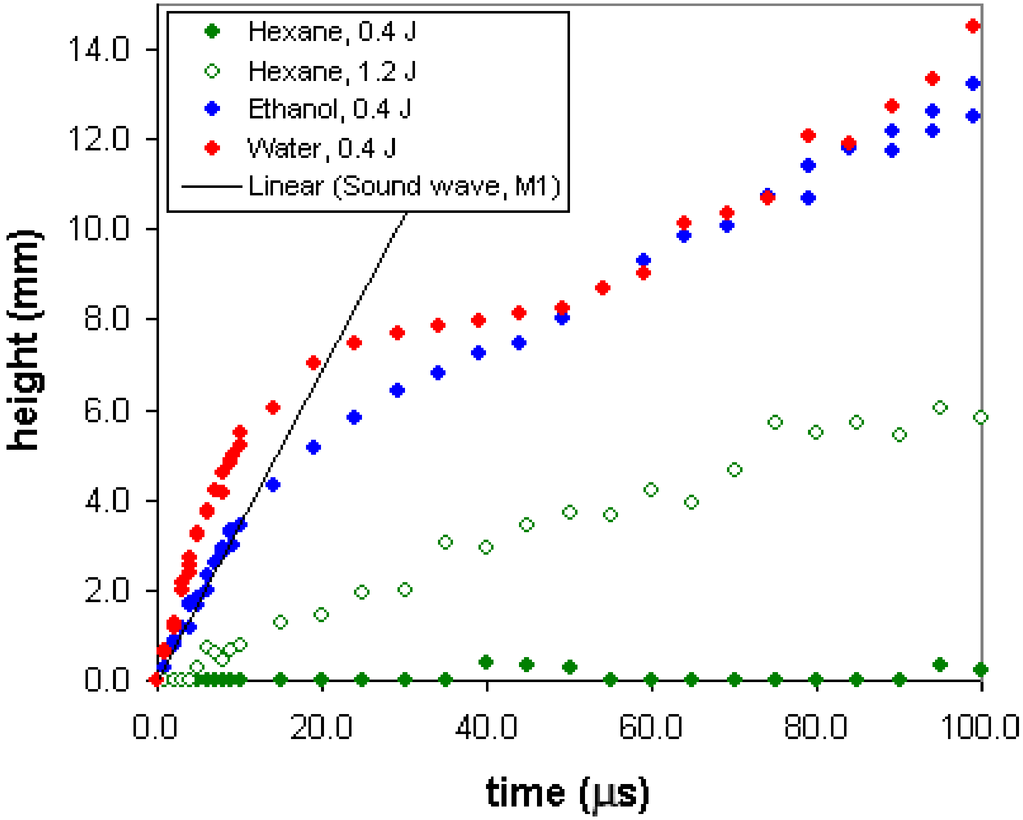

Surface absorbing liquids transonic – supersonic initial velocities observed

Volume absorbing liquids: subsonic to transonic velocities observed

Specific Impulse and Internal Efficiency

$$I_{sp} \equiv \frac{I}{w} \approx \frac{u_e}{g}$$

(1.6×10^7 W/cm^2, 0.4 J)

Specific Impulse (s)	Hexane	Ethanol	Water
from v_0/g	-	42 ± 1	84 ± 3
1st 100 μs	-	10 ± 5	20 ± 10
Total process	2.3 ± 0.6	0.40 ± 0.05	0.34 ± 0.05

Internal Efficiency (%)	Hexane	Ethanol	Water
from v_0/g	-	10.3 ± 0.7	18 ± 2
1st 100 μs	-	3 ± 1	4 ± 2
Total process	0.24 ± 0.08	0.10 ± 0.01	0.07 ± 0.01

UAH
The University of Alabama in Huntsville

Force Data with ICCD Imaging

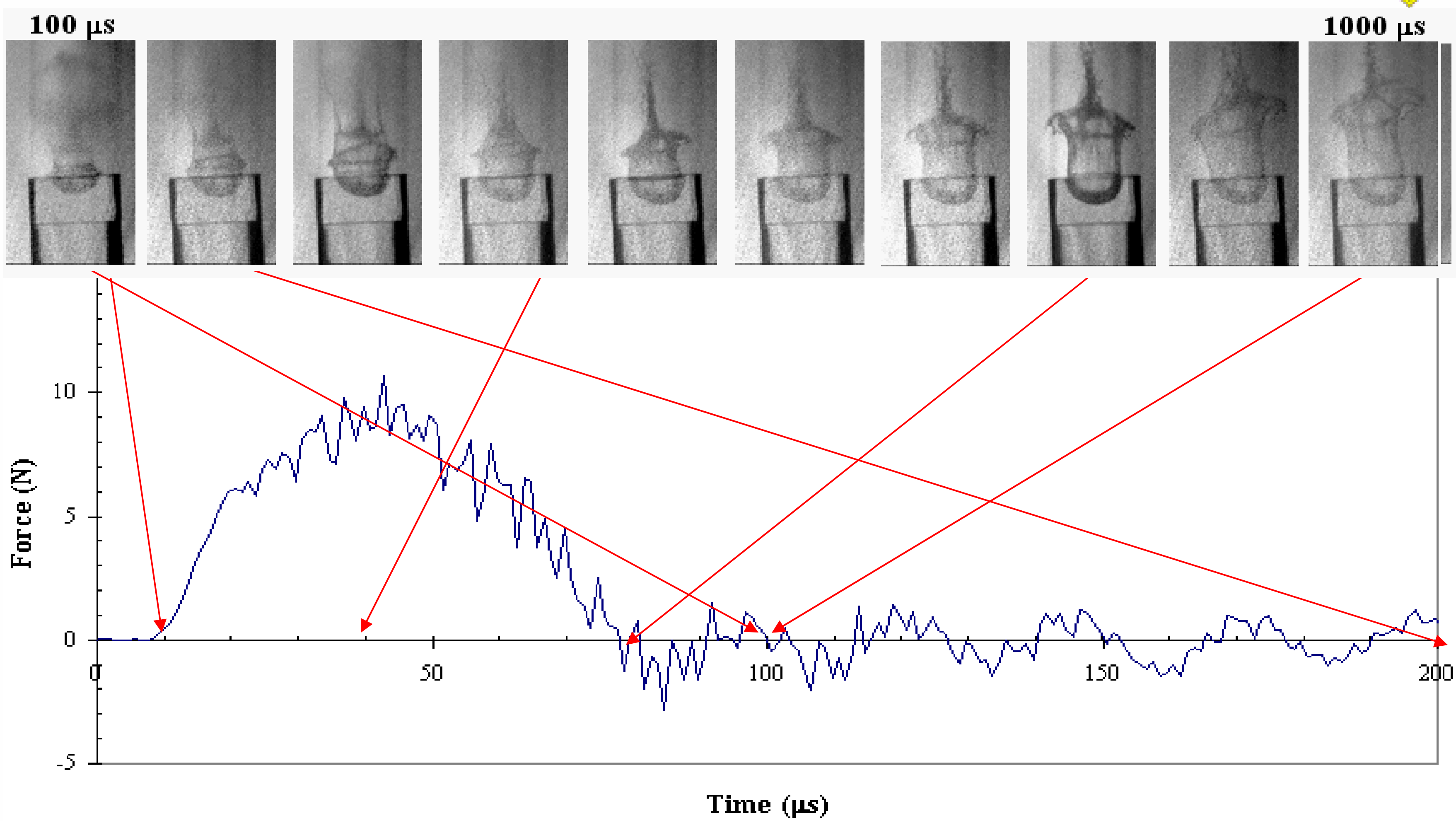

(Water, cylinder, concave, 0.4 J, 4 x 10^7 W/cm^2)

Conclusions

Conclusions

1) A series of experiments with time-resolved force sensors and ICCD imaging were conducted on liquids.
2) 2 major physical ablation processes are observed: vaporization and splashing. In some cases plasma formation was also achieved.
3) The major source of thrust generation in the laser ablation of liquids is vaporization.
4) ICCD imaging shows vaporization occurs from 0 to 100 μs after the laser pulse. Splashing is initiated after about 100 μs.
5) Force generation occurs during the vaporization regime.
6) The peak force was observed ~40-50 μs after the laser pulse.
7) Ballistics experiments corroborate the impulse measurements with force sensors.
8) Surface absorbing liquids show higher C_m (~50-150 dyne/W) than volume absorbing liquids (~10-50 dyne/W).

Conclusions (continued)

9) C_m is dependent on surface geometry for surface absorbing liquids. Changing geometry does not affect C_m for volume absorbing liquids.
10) C_m is dependent on container geometry for volume absorbing liquids. Changing container geometry does not affect C_m for surface absorbing liquids.
11) The majority of mass loss occurs due to splashing (>95%) rather than vaporization (<5%).
12) Momentum coupling was observed to be about 3 times more sensitive to changes in the surface curvature for surface absorbing liquids than to changes in the container geometry for volume absorbing liquids. This is additional evidence in favor of a dominant vaporization mechanism.

THANK YOU

This presentation is Distribution A: Approved for public release, distribution unlimited

Cavity Growth

- 2 Regimes:
  - Approximately linear growth
  - Vaporization – fast growth
  - Splashing – slow growth

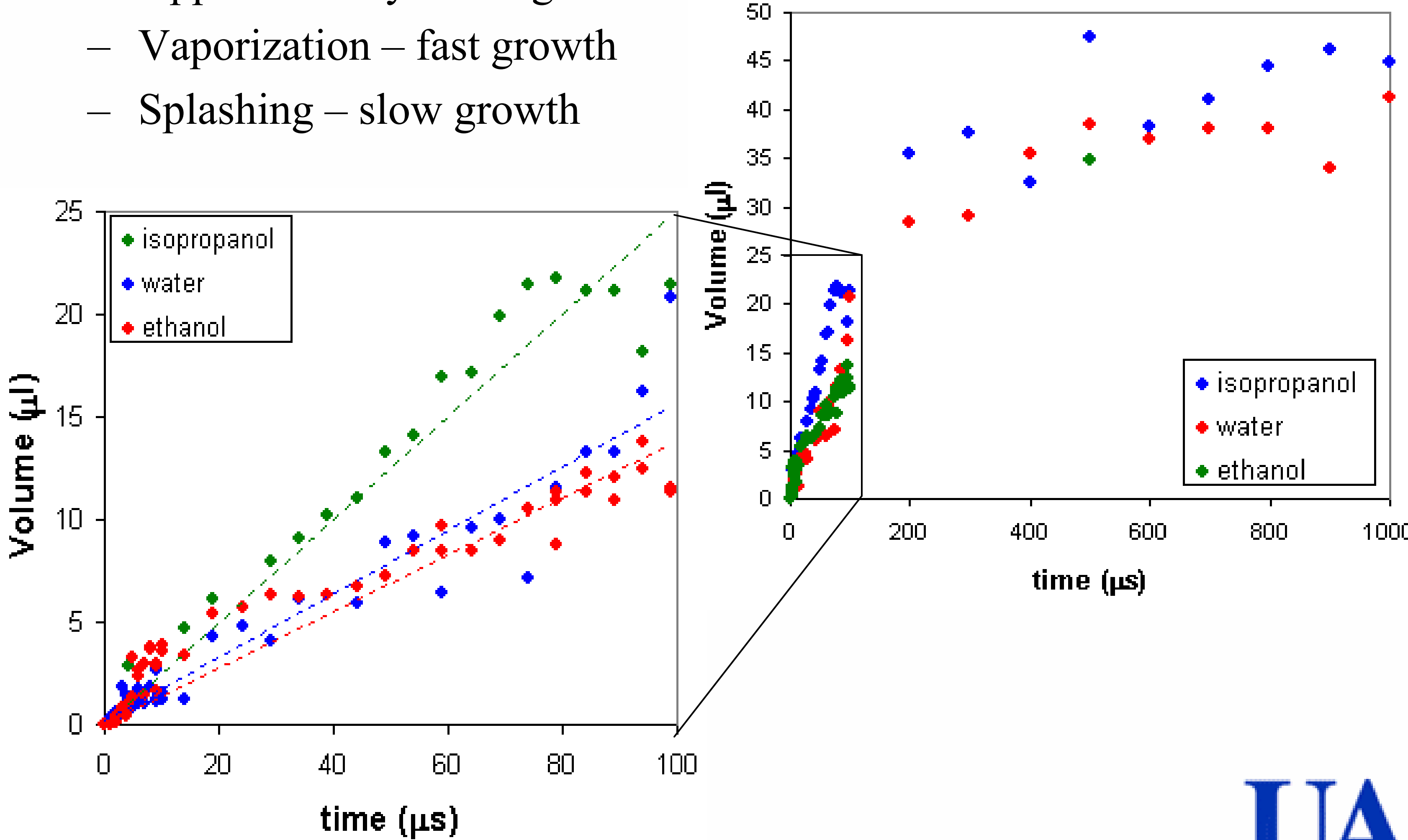

Challenges of Using Piezoelectric Force Sensors

- Measurements in an accelerating frame
  - Distortion*
  - Solution: Sensor at rest
- Rise time limits detection speed
  - Plasma processes ~ 1 μs
  - Liquid vaporization ~ 100 μs
  - Cavity Collapse ~ 1 ms
  - Liquid splashing ~ 10 ms

  (Force sensors: 5 μs rise time)
- Natural frequencies
  - Solution: Fourier analysis

Drag vs. Velocity

Coefficient of Parasite Drag Vs. Velocity

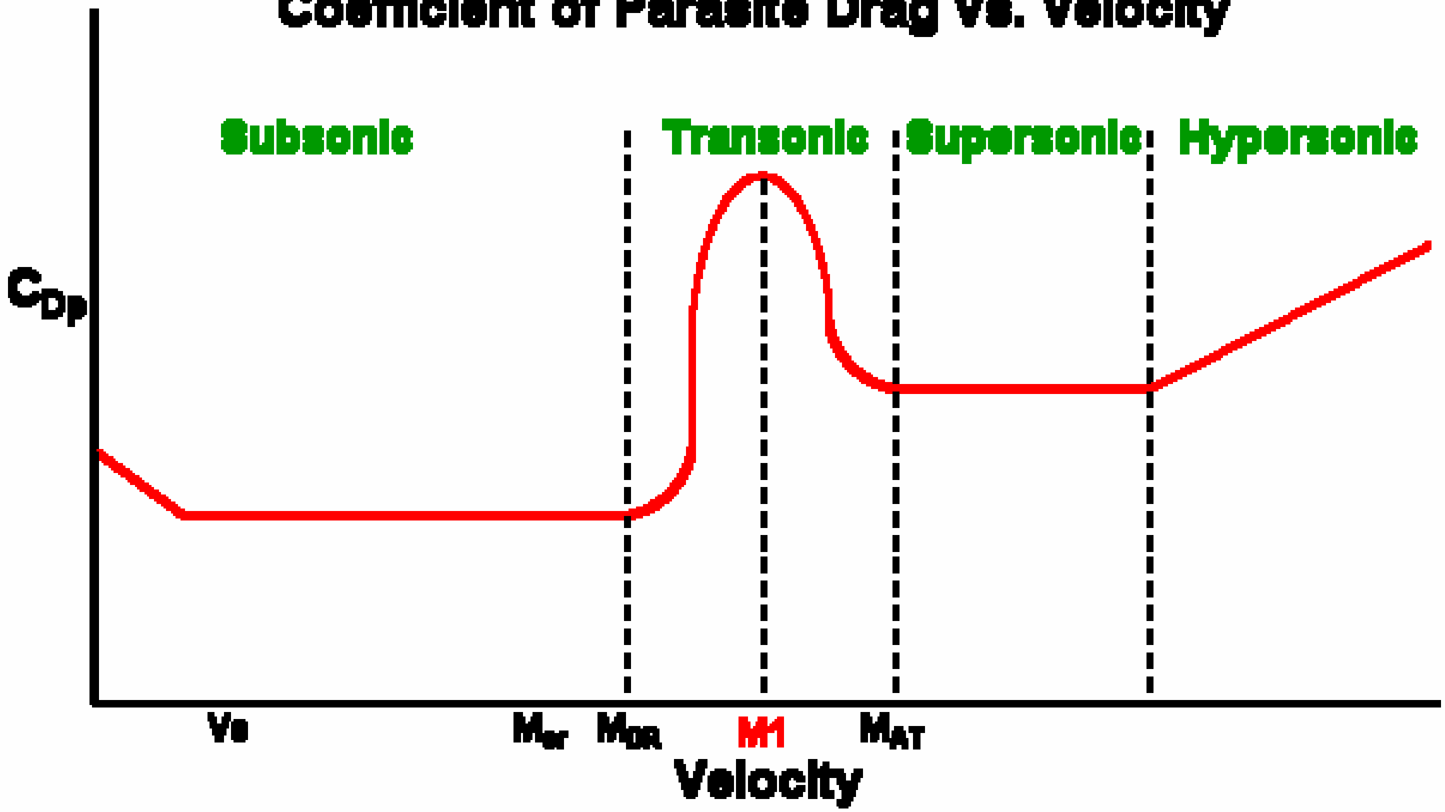

UAH
The University of Alabama in Huntsville

Force Sensor Distortion

- Spring mounted vs. Hard mounted sensor

back

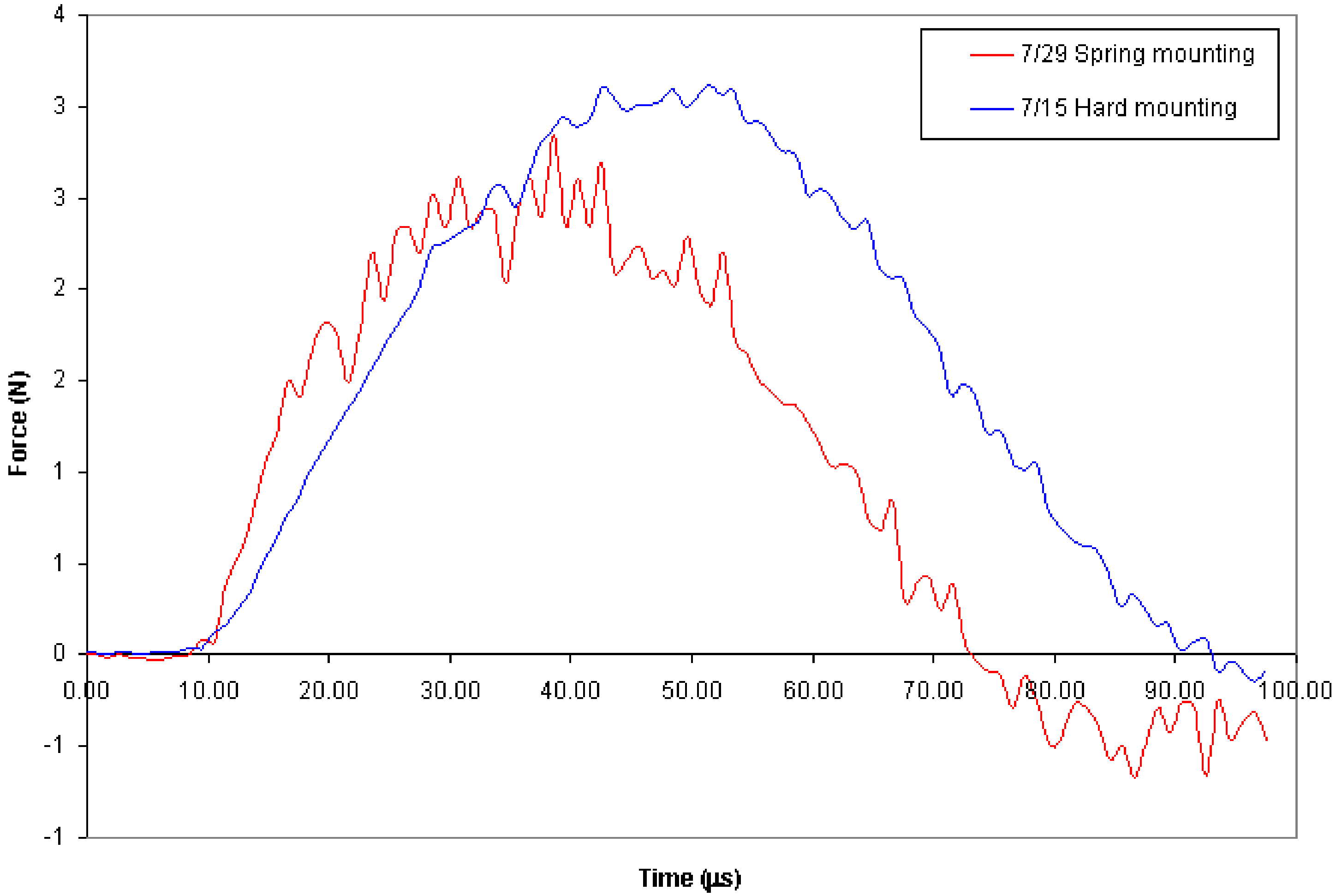

This presentation is Distribution A: Approved for public release, distribution unlimited

Laser Properties

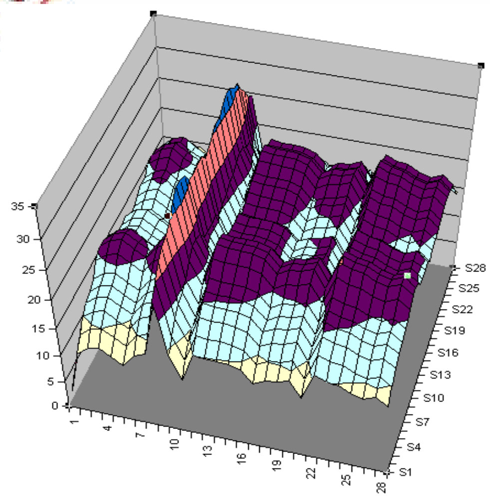

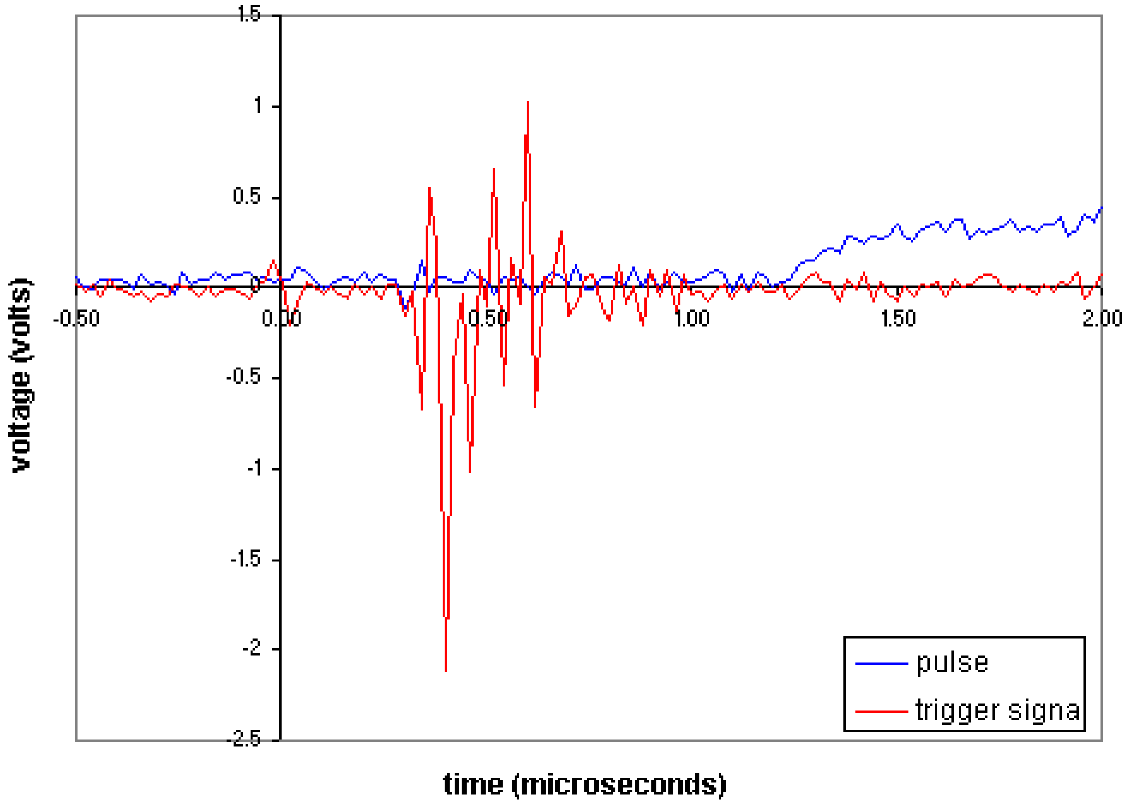

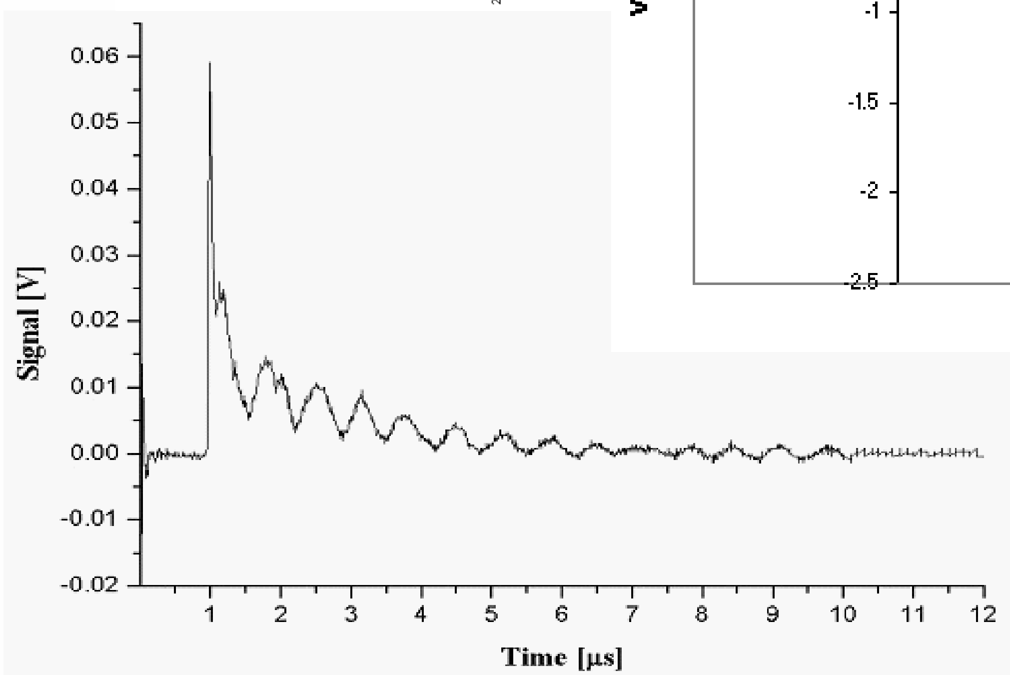

Liquids

	Hexane	Ethanol	Isopropanol	Acetone	Water
Chemical Formula	C_6H_{14}	C_2H_5OH	C_3H_7OH	C_3H_6O	H_2O
Absorption Coefficient (cm^{-1})	~0	17	67	~100	~3300
Absorption Depth (μm)	large	574	149	78	3
Density (g/ml)	0.66	0.79	0.785	0.790	1.0
Molecular Weight (g/mol)	86.18	46.07	60.10	58.08	18.02
Enthalpy of Vaporization (kJ/mol)	28.85	38.6	39.85	29.1	43.99
Surface Tension (dyne/cm)	18	22.3	21.7	23.7	73.05
Viscosity (mPa-s)	0.3	1.07	2	0.306	1.002

Quartz Target Containers

Cone

Cylinder

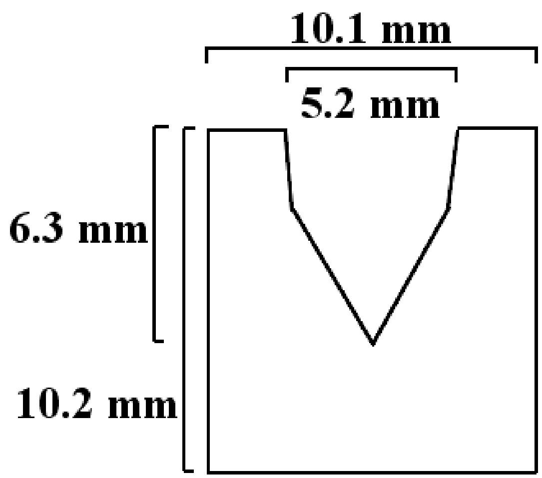

1.672 g
67.5 μl

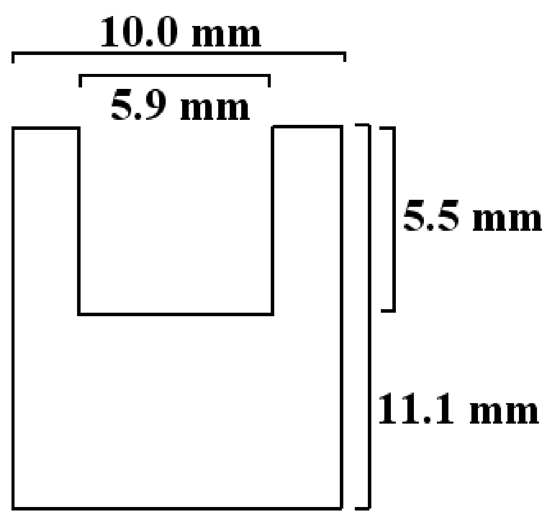

1.601 g
146.9 μl

Surface Distortion

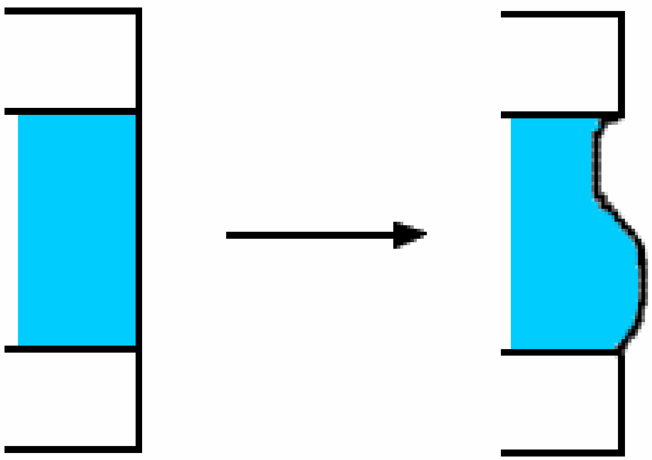

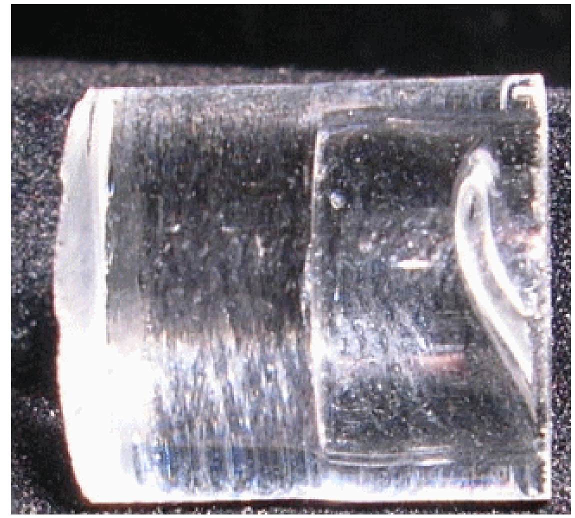

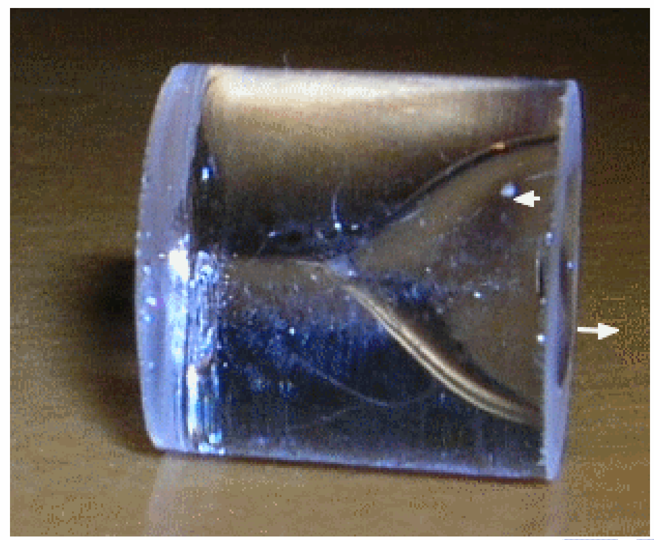

UAH
The University of Alabama in Huntsville